

# RSC Advances



This is an *Accepted Manuscript*, which has been through the Royal Society of Chemistry peer review process and has been accepted for publication.

*Accepted Manuscripts* are published online shortly after acceptance, before technical editing, formatting and proof reading. Using this free service, authors can make their results available to the community, in citable form, before we publish the edited article. This *Accepted Manuscript* will be replaced by the edited, formatted and paginated article as soon as this is available.

You can find more information about *Accepted Manuscripts* in the [Information for Authors](#).

Please note that technical editing may introduce minor changes to the text and/or graphics, which may alter content. The journal's standard [Terms & Conditions](#) and the [Ethical guidelines](#) still apply. In no event shall the Royal Society of Chemistry be held responsible for any errors or omissions in this *Accepted Manuscript* or any consequences arising from the use of any information it contains.

**Preservation of biomacromolecular composition and ultrastructure of decellularized  
cornea using perfusion bioreactor**

Sharda Nara, Shibu Chameettachal, Swati Midha, Sumit Murab, Sourabh Ghosh\*

Department of Textile Technology, Indian Institute of Technology, New Delhi, India

\* Corresponding author

Dr. Sourabh Ghosh

Associate Professor

Department of Textile Technology,

Indian Institute of Technology Delhi

Hauz Khas, New Delhi- 110016

India

Email: sghosh08@textile.iitd.ac.in

Phone: 91-11-2659-1440

Fax: 91-11-2659-1103

**Abstract:**

An attempt has been made to formulate a new method of corneal decellularization using a direct perfusion system through the cornea. Here, we compared the direct perfusion method to some commonly used decellularization strategies including chemical methods; non-ionic detergent TRITON X-100 and ionic detergent; sodium dodecyl sulphate (SDS) based orbital shaker method and physical methods of liquid nitrogen and freeze-thaw to decellularize goat cornea. Histochemical evaluation and biochemical estimation highlighted that liquid nitrogen, freeze-thaw and TRITON- based orbital shaker methods resulted in incomplete removal of resident cells from native cornea. On the contrary, direct perfusion of cornea using TRITON and SDS completely removed all the cells from the cornea while preserving the ultrastructure of the extracellular matrix at a steady flow rate of 10  $\mu\text{l}/\text{min}$ . Raman and ATR-FTIR spectra indicated the relative abundance of  $\alpha$ -helical conformation of collagen type I in perfused cornea while  $\beta$ -sheet conformation was predominantly observed in other treatment methods. FACS was used to determine the cell death modality in different methods of decellularization. In direct perfusion system, 13.1% higher apoptotic cells, the preferred route of cell death, were observed in cornea compared to orbital shaker-based methods. Further, feasibility studies conducted for 7 days to investigate the recellularization potential of perfused decellularized matrix demonstrated well attached viable population of seeded corneal stromal cells. In summary, we demonstrated that direct perfusion method for decellularization of cornea using 0.1% TRITON detergent at 10  $\mu\text{l}/\text{min}$  is an optimal strategy for efficiently removing the resident corneal cells while maintaining the

ultrastructure of the corneal matrix intact and therefore could serve as an excellent source for corneal transplantation.

**Keywords:**

Decellularized cornea, direct perfusion, spectroscopic tools, extra cellular matrix, recellularization.

## Introduction

Cornea, being the outermost layer of the eye is highly prone to trauma associated injuries. For severe injuries, surgical procedures including penetrating keratoplasty and partial thickness keratoplasty, such as Descemet's stripping, endothelial keratoplasty are the major treatment options for corneal blindness.<sup>1</sup> However a major drawback with these methods is the requirement for fresh cadaveric tissue. To circumvent the shortage of donated cornea, tissue engineered cornea<sup>2</sup> or xenografts<sup>3</sup> are being investigated as suitable alternatives. Decellularization of whole organs such as the lungs,<sup>4</sup> heart<sup>5</sup> and liver<sup>6</sup> led to the development of constructs for transplantation. Extrapolation of these studies led to the hypothesis that decellularized cornea generated by removing cells from a cadaveric cornea may provide an ideal biological matrix for developing corneal tissue constructs. Recent reports have shown that decellularized corneal tissue transplanted as a graft can serve as a substrate for cultured corneal keratocytes as well as endothelial cells as the tissue carries the preserved extracellular matrix (ECM),<sup>7</sup> which is difficult to fabricate using synthetic materials.

Structural and functional maintenance of the ECM architecture, including the alignment of fibrous proteins and preservation of glycosaminoglycan (GAG) molecules are vital to the transparency and biological functionality of the corneal tissue.<sup>8</sup> The uniformly parallel alignment of the bundle of collagen fibrils (arranged in 200–250 nm thick orthogonally stacked lamellae), mainly comprising of collagen type I (Col I) (80%) and Col V (20%), is indispensable for maintaining corneal tissue transparency and is therefore an extremely crucial consideration in devising protocols for

decellularization.<sup>9,10</sup> The regenerative mechanisms induced by decellularized ECM are not just regulated by specific “organomorphic” structures, but are significantly affected by the physiological presentation of regulatory molecules exposed by the 3D tissue microenvironment. The decellularized ECM could be exploited to guide the proliferation and differentiation of cultured keratocytes/endothelial cells towards recellularizing the matrix by applying the principles of morphogenesis.<sup>11</sup> Hence the main challenge in decellularization of corneal tissue is developing an ECM comprising of an intact arrangement of collagen fibres and corneal proteoglycans including glycosaminoglycans (keratan sulphate and dermatan sulphate) that would possess the morphogens while also providing a substrate for corneal cell culture by guiding the shape and stability of tissues *via* precisely regulating cell-ECM and cell-cell communication.

Several methods of decellularization have already been postulated for corneal decellularization, including the use of detergents such as sodium dodecyl sulphate (SDS)<sup>12</sup> and TRITON X-100 (t-octylphenoxypolyethoxyethanol),<sup>4,13</sup> enzymes such as phospholipase A2,<sup>14</sup> high hydrostatic pressure<sup>15</sup> and gaseous nitrogen.<sup>16</sup> But none of these methods have been able to achieve complete removal of cellular fragments while keeping the intrinsic structure and precise alignment of the constituent fibrous ECM intact. Therefore combination strategies were applied, for instance, Luo and co-workers<sup>17</sup> demonstrated complete decellularization of porcine cornea by using a combination of 0.2% TRITON and mild salt solution (2M NaCl). Moreover, such decellularized cornea showed successful recellularization with multi-layered stratification with rabbit amniotic endothelial cells and successfully healed an alkali burn in rabbit lamellar keratoplasty. However, the procedures were lengthy and required a combination of techniques; no

single technique could completely remove the cells along with debris.<sup>17</sup> Instances where singular techniques were applied for decellularization of tissues, higher concentration solutions, such as 2% TRITON<sup>7</sup> or 0.5% SDS<sup>12</sup>, were used which proved to be detrimental for the preservation of the ECM ultrastructure.

Therefore another important consideration is the type of detergent (ionic or nonionic) and its concentration which may inflict different extents of damage on the treated corneal tissues. Ionic detergents (such as SDS) were found to be more effective over non-ionic detergents (such as TRITON) in case of perfusion-based decellularization studies conducted on liver, lungs and heart.<sup>5-7</sup> However, reported literature confirms extensive matrix protein damage in SDS-treated corneas<sup>18</sup> over TRITON.<sup>19</sup> Hence, there is a need to optimize the application of mild detergents which can effectively be utilized towards decellularization of corneal tissues without damaging the underlying ECM architecture to open up new possibilities for decellularization strategies.

Compared to simple immersion in decellularizing fluid,<sup>20</sup> perfusion strategies such as passing the detergent through the native vascular system<sup>6</sup> was found to be advantageous. Complex perfusion systems, designed for large tissues, comprise of multiple peristaltic pumps and the liquid perfusion is regulated by various valves placed in all the connections.<sup>5-7</sup> In this study, we hypothesized that a relatively simple perfusion based strategy, directly through the cornea, with precisely regulated flow rate, would be suitable for corneal decellularization over other conventional methods.

In the present study, the goat corneal tissue was decellularized by direct perfusion based strategy using 0.1% TRITON at varied flow rates (10-100  $\mu$ l/min). In order to

evaluate the efficiency of direct perfusion based strategy, we have compared the results with other conventional methods including chemical methods using SDS, TRITON at different concentrations 0.1%, 0.5% in orbital shaker and physical methods including liquid nitrogen and freeze-thaw. Spectroscopic tools such as Raman and ATR-FTIR were employed to examine the secondary conformation of collagen in each case and interpret the damage caused by the use of different decellularization protocols. The spectra of the decellularized matrices were further correlated with histological and biochemical analysis. Further, flow cytometric analysis was carried out to study the cell death modalities in the tissues during decellularization. At the end, the most optimally decellularized matrix with intact ECM ultrastructure was subsequently recellularized with corneal stromal cells and cultured in dynamic conditions for 7 days to test their feasibility towards developing corneal constructs.

## **2. Experimental Section**

### **2.1 Preparation of decellularized goat corneal matrix**

Cadaveric goat eyes were provided by All India Institute of Medical Sciences, New Delhi, India with prior approval from the Institute Ethics Committee. The goat corneas were excised from the ocular globe under sterile conditions and washed several times in PBS (pH 7.2-7.4) containing 100 U/ml penicillin-streptomycin (Lonza, U.S.A), 50 µg/ml gentamycin (Himedia, India) and 100 µg/ml amphotericin B (Himedia, India) (antibiotic mixture).



To obtain the most efficient method of cornea decellularization, a comparative study between the four methods including physical (liquid nitrogen and freeze thaw) and chemical methods (TRITON and SDS) was conducted. A schematic representation of the various methods employed has been illustrated in **Fig. 1**.

### 2.2.1 Chemical methods

The various experimental parameters for the two chemical methods; orbital shaker and direct perfusion are illustrated below in **Table 1**.

**Table 1:** Summary of different conditions used for chemically decellularizing cornea.

Method	Detergent		Process parameters	Time
Orbital Shaker	TRITON	SDS	speed of shaker: 40 rpm	24 h
	0.1%, 0.5%	0.1%, 0.5%		
Direct perfusion	TRITON 0.1%		flow rate of detergent: 10, 50 & 100 $\mu$ l/min	24 h

#### Orbital Shaker

For comparing the most suitable chemical method for decellularization, the goat corneas were immersed in TRITON X-100 (Fisher Scientific, India) or SDS (Merck, India) in 0.1% (v/v) and 0.5% (v/v) concentrations of both the detergents. Each experimental group comprised of 3 corneas. Native untreated corneas were used as controls (n = 3). All detergent solutions were prepared in PBS with a solvent/tissue mass ratio of 20:1 (v/wt). The corneas, immersed in the respective detergent solutions were

placed in 20 ml beakers in an orbital shaker (JULABO, Germany) at 40 rpm for 24 h and 25°C. Finally, the samples were rinsed in antibiotic mixture for another 48 h at 40 rpm with PBS changed every 2 h.

### **Direct perfusion of detergent for decellularization**

Removal of corneal cells from the dissected tissue was performed using a perfusion chamber (kindly provided by Prof Ivan Martin, Basel, Switzerland) as described elsewhere<sup>21,22</sup> Briefly, TRITON was perfused directly through the corneal tissue (n = 3) using a syringe pump (Kd Scientific, USA) unidirectionally in the flow range of 10 to 100 µl/min for 3 sets (10, 50 and 100 µl/min) maintaining a continuous flow rate for 24 h. Subsequently, the decellularized tissue was rinsed by perfusing antibiotic mixture at a flow rate of 10 µl/min for 24 h.

### **2.2.2 Physical methods**

Liquid nitrogen and freeze-thaw methods were employed to physically remove cells from the cadaveric goat cornea. The basic principle behind physical processing is that rapid cooling causes effective lysis of the resident cells by disruption of the cell membrane due to the intracellular formation of ice crystals.

#### **Liquid Nitrogen**

The dissected corneas (n = 3) were placed in separate cryogenic vials and frozen in liquid nitrogen for 4 h. Following freezing, the tissue samples were rinsed in sterile PBS supplemented with antibiotic mixture for another 48 h at 40 rpm with PBS changed every 2 h, as described above. Native untreated corneas (n = 3) were used as controls.

**Freeze-thaw:**

The dissected goat corneas were placed in microfuge tubes at -20°C for 2 h subsequently followed by rapid thawing at RT. This freeze-thaw cycle was repeated for 48 h, followed by rinsing with antibiotic mixture to remove the residual cell remnants. The experiment was performed in triplicate and untreated corneas were used as controls.

**2.3 DNA quantification**

DNA was isolated from both native and decellularized goat corneas (n=3) using DNA extraction kit (Agilent Technologies, Germany, Cat. no. 200600-1) according to manufacturer's guidelines. Quantification was performed on a spectrophotometer (Thermo Scientific NanoDrop 2000c, USA).

**2.4 Histological evaluation**

For light microscopy, native and treated corneas (of both physical and chemical methods) were fixed in 4% formaldehyde (Merck, India) for 4 h, washed with PBS, dehydrated in graded alcohol series and subsequently embedded in paraffin. For histological staining, 6 µm thick sections were stained with hematoxylin and eosin (H&E) and examined under a light microscope.

For nuclear staining, the paraffin sections were dewaxed in xylene and immersed in 0.1% TRITON (v/v) diluted in PBS for 2 min. After three consecutive washes in PBS, the specimens were treated with 10 % bovine serum albumin for 1 h at 37 °C and subsequently stained with 4',6'-diamidino-2-phenylindole (DAPI) for 2 min at RT for nuclear staining. Finally the specimens were washed thoroughly in PBS and mounted on

glass slides. The images were captured under a fluorescence microscope (Leica DFC295, Germany) using Leica software application suite (LAS V3.8).

## 2.5 Glycoaminoglycan (GAG) quantification

Residual GAG content in the decellularized corneal tissues (processed using both chemical and physical methods) was estimated by dimethyl methylene blue (DMMB) assay with chondroitin sulfate (Himedia, India) standard. The sections were subjected to enzymatic treatment by immersing in 500  $\mu$ l of proteinase K (SRL, India) overnight at 56°C. The digested portions of the tissue were analyzed to quantify GAG. Measurements were normalized to dry weight of the tissue. The spectrophotometric readings were taken at 525 nm using a microplate reader (BIORAD iMark microplate reader, USA).

## 2.6 Flow Cytometry Analysis (FACS)

For FACS, partially decellularized tissues were obtained by subjecting the goat corneas to different decellularization protocols including liquid nitrogen, freeze thaw, TRITON (0.1%) orbital shaker and TRITON (0.1%) direct perfusion for 2 h. The same concentration and detergent type were taken for both methods (orbital shaker and direct perfusion) in order to evaluate the effect of different techniques on cell death modalities. In order to ascertain the mechanism of cell death (apoptosis or necrosis) during decellularization, cells were extracted from partially decellularized cornea using previously described protocol,<sup>21</sup> used for isolating cells from 3D constructs. Briefly, the tissues were subjected to enzymatic treatment *via* perfusion with 0.03% collagenase type I (wt/v) diluted in PBS continuously for 45 min at a flow rate of 1 ml/min, followed by perfusion with 0.5% trypsin for 15 min while maintaining the same flow rate. The

harvested cells were centrifuged at 1500 rpm for 5 min, washed twice with PBS, counted with Neubauer chamber and characterized by flow cytometry. Flow cytometry was performed using FITC Annexin V Apoptosis Detection Kit I (BD Pharmingen™ Cat. no. 556547). Harvested cell suspensions ( $\leq 20,000$  cells per sample) obtained from partially decellularized tissues were stained with FITC Annexin V and propidium iodide (PI) and incubated for 30 min at 4°C. An untreated population of cells was maintained so that the basal level of apoptotic and necrotic cells might be defined.

The extent of apoptosis was determined by subtracting the percentage of apoptotic cells in the untreated population from the treated population. Positive controls included in the study were heat shock treated cells for necrosis,<sup>23</sup> whereas UV treated cells for apoptosis.<sup>24,25</sup> For flow cytometric analysis, a system (BD FACSCalibur, USA) equipped with a single Argon ion laser was used at 488 nm excitation wavelength of and emission filters at 515-545 BP (green; FITC) and 600 LP (red; PI). Electronic compensation was used to prevent bleed through of fluorescence. Data analysis was performed using BD FACStation software.

## **2.7 Attenuated total reflectance – Fourier transform infrared spectroscopy (ATR-FTIR)**

ATR-FTIR spectra of freeze dried goat corneas were obtained using a spectroscope (Bruker Alpha-P, USA). All the spectra were observed in the range of 2000 to 500  $\text{cm}^{-1}$  at data acquisition rate of 4  $\text{cm}^{-1}$  per point in absorbance mode with 50 scans taken for each sample, followed by spectra analysis for relative comparison.

Deconvolution and curve fitting were performed on the average spectra using automated Peakfit version 4.1 software (SeaSolve software Inc., USA).

## 2.8 Raman Spectroscopy

For Raman spectra of decellularized, freeze dried corneas were obtained using a confocal laser dispersion Micro-Raman spectrometer (inVia reflex, UK) system equipped with a 785 nm diode laser and integrated with FTIR IlluminatIR II™ module. This system was combined with Leica microscope to allow scatter, line, area mapping and confocal depth profiling. All Raman measurements were taken at 50 X magnification. The samples were placed on aluminium slides and measurements were taken on 5 randomly selected points per sample with an integration time of 10 seconds.

## 2.9 Measurement of transmittance

Initially the transparency of each sample was visually estimated. Subsequently, in order to validate these findings, the transmission spectra of decellularized as well as the untreated samples were observed using a UV-Vis-NIR spectrophotometer (Perkin Elmer, U.S.A). The spectral distribution was measured in the 400-800 nm spectral range.<sup>26</sup> The thickness of each sample was determined by light microscopy (Leica DFC295, Germany) and the results were normalized with respect to native tissue.

## 2.10 Orientation of collagen fibres

The orientation of collagen fibres in the differently decellularized corneal matrix was analyzed from H&E stained light micrographs by using orientationJ software.<sup>27</sup> The

coherency coefficient of different regions was depicted by red ellipses inside the yellow region of interest.

## **2.11 Cell Culture**

### **2.11.1 Explant culture**

Goat cornea was isolated from the ocular globe by removing the sclera, soft connective tissue and the limbal rings. After separating the three layers carefully, the stromal layer was cut into small pieces of approximately 2-3 mm and washed extensively with antibiotic mixture. After thoroughly rinsing with PBS, the fragmented tissue pieces were carefully lifted using sterile forceps and incubated at the bottom of a T25 tissue culture flask for 7 days in DMEM (CELLclone™, India)

The freshly isolated goat corneal stromal cells were expanded in DMEM with 10% fetal bovine serum (Biological Industries, India) and 100U/ml penicillin-streptomycin. For serial passaging, cells were washed with 1X PBS and dissociated using 0.25% trypsin (v/v) (Lonza, U.S.A) diluted in PBS. Standard culture conditions of 5% CO<sub>2</sub> and 95% humidity at 37°C were maintained.

### **2.11.2. Fabrication of porous decellularized corneal scaffold**

The decellularized corneal matrix obtained after direct perfusion protocol was further processed for cellular re-seeding. The freeze dried decellularized corneal scaffolds (n=3), containing pores of different sizes were fabricated at a pre-freezing temperature of -20°C.<sup>14</sup> A scanning electron microscope (SEM, EVO 50, Zeiss, UK) was used to analyze

longitudinal sections of freeze dried cornea and a total of three micrographs per sample were obtained to measure the respective pore diameters using ImageJ software.

### **2.11.3. Recellularization of porous freeze dried cornea**

For re-seeding the tissue with freshly isolated stromal cells, decellularized matrix (size 5×5 mm with thickness of 2.5 mm) was extensively treated with antibiotic mixture. Re-seeding and subsequent cell culture was carried out using the perfusion bioreactor, pursuing the same protocol as described elsewhere.<sup>21,22</sup> Briefly, the cell suspension having  $1 \times 10^6$  cells/ml was continuously perfused through porous freeze dried decellularized matrix in alternate directions for 3 days. Then the cell suspension was completely replaced with cell free fresh media which has been perfused for 4 days. After 7 days of dynamic culture, the tissue was fixed for histological analysis.

To evaluate the recellularization efficiency, histological images corresponding to anterior and posterior portions of stromal region were obtained using light microscope (Leica DFC295, Germany) and the number of keratocytes were determined per field.

### **2.12 Statistical analysis**

Statistical comparisons were conducted by the Student's t test. Results with  $p \leq 0.05$  were considered to be statistically significant. The data pertaining to DNA and GAG quantification was expressed as mean value  $\pm$  standard deviation.

## **3 Results**

### **3.1 Histological examination**



Histological analysis of decellularized corneas processed by different methods has been illustrated in **Fig. 2**. The physical methods of decellularization including liquid nitrogen (**Fig. 2 a1-a3**) and freeze-thaw (**Fig. 2 b1-b3**) did not yield completely decellularized ECM matrix as evidenced by the presence of cellular nuclei of the resident cells distributed throughout the stroma. Further to this, treatment with TRITON in an orbital shaker (**Fig. 2 e,f**) showed similar results to the physical methods (**Fig. 2 a,b**) with incomplete removal of the resident cells (**Table 2**). On the contrary, other chemical approaches including treatment with SDS detergent in orbital shaker (**Fig. 2 c,d**) and direct perfusion with 0.1% TRITON (**Fig. 2 g-i**) were able to remove the entire resident cell population with no visible nuclear debris remaining. Decellularization using the above chemical methods was successfully achieved irrespective of the detergent concentration or the perfusion flow rates listed in **Table 1**. Amongst the two detergents used, TRITON in direct perfusion method was seen to have least deleterious effects on the structure and orientation of the collagen fibrils (**Fig. 2 g-i**). Moreover, gross preservation of the ultrastructure of Descemet's membrane (evident by the presence of the fibrous nature of the tissue) and Bowman's membrane were evident from H&E micrographs. On the other hand, the collagen architecture was found to be partially disorganized within the corneal stroma after being treated with SDS (**Fig. 2 c,d**).

Though complete decellularization of the corneal specimens was observed at all the given flow rates (**Table 1**), 10  $\mu\text{L}/\text{min}$  was considered as the most optimal flow rate used for direct perfusion due to minimal evidence of deterioration observed in the resultant tissue structure (**Fig. 2 g1-g3**). A partial disruption in the Bowman's and Descemet's membrane was visible at 50  $\mu\text{L}/\text{min}$  (**Fig. S1 a1,a2**), however, both the

corneal membranes were completely removed when flow rate was increased further to 100  $\mu\text{l}/\text{min}$  (**Fig. S1 b1,b2**). A logical explanation could be that higher flow rates generate extra shear stress on the tissue subsequently resulting in the removal of the Descemet's membrane along with the resident cells.

### 3.2 Biochemical analysis

Biochemical analysis was performed to quantify the GAG and DNA content of the decellularized corneas processed by different methods. Unprocessed native cornea was used as control for the study. Significant differences in the DNA content were observed in all the different decellularization protocols with respect to each other. Native, unprocessed cornea showed the highest levels of GAG ( $35 \pm 0.1 \mu\text{g}/\text{ml}$ ) and DNA ( $185 \pm 0.2 \text{ ng}/\text{mg}$  dry wt.) content compared to all the decellularized corneal matrices ( $p < 0.05$ ) (**Fig. 3**). Whereas, lowest DNA ( $10 \pm 0.4 \text{ ng}/\text{mg}$  of dry wt.) was observed in SDS treated cornea (**Table 2**) as compared to all the other treatments. However, simultaneous reduction of GAG content to  $13 \pm 0.4 \mu\text{g}/\text{ml}$  made this procedure less suitable for generating decellularized corneal matrix. For physical methods, the residual DNA content in both liquid nitrogen and freeze-thaw procedures was more than 50  $\text{ng}/\text{mg}$  dry wt., which exceeds the ideal range of decellularized matrix,<sup>28</sup> hence the results indicated partial decellularization of the corneal matrix in both the physical methods. In chemical methods, orbital shaker using higher concentration of TRITON (0.5%) showed  $50 \pm 0.9 \text{ ng}/\text{mg}$  of dry wt. of DNA and  $14 \pm 0.5 \mu\text{g}/\text{ml}$  GAG content. On the other hand, substantially reduced levels of DNA ( $20 \pm 0.2 \text{ ng}/\text{mg}$  dry wt. of tissue) and relatively higher GAG content ( $27 \pm 0.7 \mu\text{g}/\text{ml}$ ) was achieved using a much lower concentration of TRITON (0.1%) in direct perfusion over orbital shaker ( $p < 0.05$ ). The reduction in GAG

content was only one fold with respect to native cornea after treatment with direct perfusion, indicating the intactness of the corneal tissue and preservance of the essential biological moieties along with complete cellular removal.

In summary, GAG content decreased significantly between the different conditions with maximum decrease seen in the case of SDS (0.1%) orbital shaker and minimal decrease in direct perfusion. However, no significant difference in the GAG content was observed in the freeze thaw and TRITON (0.5%) orbital shaker based method.

**Table 2.** Comparison of the results obtained from decellularizing the cornea tissue by different methods.

<b>Decellularization method</b>	<b>DAPI</b>	<b>H&amp;E staining</b>	<b>GAG (µg/ml)</b>	<b>DNA (ng/mg of dry wt.)</b>	<b>Transmittance (%) at 800 nm</b>
<b>Direct Perfusion</b>	-	-	27±0.7	20±0.2	60%
<b>TRITON (Orbital shaker, 0.5%)</b>	+	+	14±0.4	50±0.9	50%

### 3.3 Attenuated total reflection – Fourier transform infrared (ATR-FTIR) spectroscopic study

ATR-FTIR spectroscopy of decellularized and native corneas was performed for analyzing the structural changes in collagen after decellularization. Amide I band (1600-1700 cm<sup>-1</sup>) appeared due to C=O bond stretching vibration. This region is sensitive to hydrogen bonding present within the protein secondary structure, thus better resolves the

collagen secondary structure viz.  $\alpha$ -helical,  $\beta$ -sheet and random coils. Amide II band appeared due to N-H bending vibration which is incapable of fully resolving the protein secondary conformation.<sup>29-32</sup> Hence amide I band ( $1700\text{-}1600\text{ cm}^{-1}$ ) was further deconvoluted to assess the structural information of collagen in the decellularized matrix.

Native cornea depicted one major peak around  $1640\text{ cm}^{-1}$  (**Fig. 4**) region whereas after deconvolution, various peaks corresponding (**Fig. 4 a1**) to  $\beta$ -sheet (22.3%),  $\beta$ -turns (37.3%), random coils (38.2%) and  $\alpha$ -helical forms (2.1%) were obtained. Native tissue was found to be predominantly  $\beta$ -sheet in structure (**Table 3**). The epithelial region of corneal tissue basically consists of Col I and IV which can be distinguished from one another based on the higher percentage of triple helix and  $\alpha$  helix as compare to  $\beta$ -sheet crystal content ( $p<0.01$ ), mainly found in Col I. On the contrary, higher  $\beta$ -sheet and lesser triple helical conformation of Col IV is attributed to its basic structural form formed of central short triple helical domain and two bulky globular terminal (N- and C-ends) domains.<sup>29</sup>

Thus the presence of  $\beta$ -sheet indicated Col IV that might be due to the presence of epithelial region.<sup>29</sup> Random coils and  $\alpha$ -helical form revealed the prevalence of Col I<sup>29</sup> in the stromal region of native cornea. Major peak position at  $1640\text{ cm}^{-1}$  was found to be similar for direct perfusion and native cornea. After deconvolution, peaks due to  $\beta$ -sheet (26.9%),  $\beta$ -turns (35.8%), random coils (14.4%) and  $\alpha$ -helical forms (22.8%) appeared in the spectra. Appearance of  $1659\text{ cm}^{-1}$  peak is due to  $\alpha$ -helical form (22.8%) (**Fig. 4 b1**, **Table 3**) indicating higher prevalence of collagen fibres consisting  $\alpha$ -helical conformation that indicated comparatively intact stromal structure.

Liquid nitrogen treated cornea exhibited one main peak around  $1629\text{ cm}^{-1}$ . In deconvoluted spectra, peaks due to  $\beta$ -sheet (68.8%),  $\beta$ -turns (16.1%) and  $\alpha$ -helical forms (18.4%) were obtained (**Fig. 4 c1, Table 3**). Here, high content of  $\beta$ -sheet (3.08 fold increase) as compared to native cornea can be seen, that might indicate collagen fibre disruption.<sup>30</sup> Further, after deconvolution  $\alpha$ -helical peak was obtained at  $1653\text{ cm}^{-1}$  thus shift of  $\alpha$ -helical peak from  $1659$  to  $1653\text{ cm}^{-1}$  also indicated some strain over collagen fibres after liquid nitrogen treatment. TRITON, 0.5% (orbital shaker) treated cornea exhibited major peak at  $1636\text{ cm}^{-1}$  and deconvoluted spectra revealed conformations of  $\beta$ -sheet (70.6%) and  $\beta$ -turns (29.4%) (**Fig. 4d1, Table 3**). In SDS, 0.1% (orbital shaker) treated cornea, main peak appeared at  $1639\text{ cm}^{-1}$  (**Fig. 4 e1**) and its deconvoluted spectra revealed peaks due to  $\beta$ -sheet (84.1%),  $\beta$ -turns (2.8%), random coils (2.8%) and  $\alpha$ -helical form (5%). Thus deconvoluted spectra depicted very high prevalence of  $\beta$ -sheet content in both of these methods. This demonstrated the conformational change of collagen secondary structure from  $\alpha$ -helical to  $\beta$ -sheet form.<sup>30</sup> Hence, orbital shaker based detergent treatment disrupt the secondary structure of collagen.

In freeze-thaw treated cornea, major peak appeared at  $1643\text{ cm}^{-1}$  (**Fig. 4 f1**) while after deconvolution, peaks appeared due to  $\beta$ -sheet (29.5%),  $\beta$ -turns (15.5%),  $\alpha$ -helical (55%) secondary conformation. The presence of  $\alpha$ -helical conformation revealed the occurrence of intact collagen secondary conformation. However, absence of peaks due to  $\beta$ -turns, random coils represents lack of transitional conformations found in native and perfused cornea. Thus, occurrence of all the peaks corresponding to  $\beta$ -sheet,  $\beta$ -turns, random coil and  $\alpha$ -helical form with predominating  $\alpha$ -helical form indicated conservation of collagen secondary structure in perfused cornea.

**Table 3.** Deconvoluted spectral peaks of amide I band (1600-1700  $\text{cm}^{-1}$ ).

Sr. No.	Tissue	Main peak	Deconvoluted peaks	Conformation (%)
1.	Native cornea	1640 $\text{cm}^{-1}$	1609.6 $\text{cm}^{-1}$ 1619.5 $\text{cm}^{-1}$ 1628.7 $\text{cm}^{-1}$ 1636.7 $\text{cm}^{-1}$ 1646.1 $\text{cm}^{-1}$ 1658.8 $\text{cm}^{-1}$ 1666.9 $\text{cm}^{-1}$ 1680.2 $\text{cm}^{-1}$	$\beta$ -turns (26.9%) $\beta$ -sheet (3.1%) $\beta$ -sheet (6.1%) $\beta$ -sheet (1.4%) random coils (38.2%) $\alpha$ -helical (2.1%) $\beta$ -sheet (11.7%) $\beta$ -turns (10.4%)
2.	TRITON, 0.1% (Direct perfusion)	1640 $\text{cm}^{-1}$	1610.5 $\text{cm}^{-1}$ 1618.1 $\text{cm}^{-1}$ 1626.7 $\text{cm}^{-1}$ 1636.4 $\text{cm}^{-1}$ 1646.6 $\text{cm}^{-1}$ 1659.5 $\text{cm}^{-1}$ 1669.1 $\text{cm}^{-1}$ 1674.9 $\text{cm}^{-1}$ 1682.5 $\text{cm}^{-1}$	$\beta$ -turns(18.5%) $\beta$ -sheet (3.2%) $\beta$ -sheet (11.6%) $\beta$ -sheet (12.1) random coils (14.4%) $\alpha$ -helical (22.8%) $\beta$ -turns (0.7%) $\beta$ -turns (6.9%) $\beta$ -turns (9.7%)
3.	Liquid Nitrogen	1629 $\text{cm}^{-1}$	1612.1 $\text{cm}^{-1}$ 1622.3 $\text{cm}^{-1}$ 1630.8 $\text{cm}^{-1}$ 1637.9 $\text{cm}^{-1}$	$\beta$ -sheet (28.6%) $\beta$ -sheet (2.4%) $\beta$ -sheet (18.1%) $\beta$ -sheet (19.7%)

			1653.6 cm <sup>-1</sup> 1662.2 cm <sup>-1</sup> 1670.8 cm <sup>-1</sup>	$\alpha$ -helical (18.4%) $\beta$ -turns (3.4%) $\beta$ -turns (9.3%)
4.	TRITON, 0.5% (Orbital shaker)	1636 cm <sup>-1</sup>	1627.9 cm <sup>-1</sup> 1665.1 cm <sup>-1</sup>	$\beta$ -sheet (70.6%) $\beta$ -turns (29.4%)
5.	SDS, 0.1% (Orbital shaker)	1639 cm <sup>-1</sup>	1618.9 cm <sup>-1</sup> 1626.6 cm <sup>-1</sup> 1628.5 cm <sup>-1</sup> 1637.7 cm <sup>-1</sup> 1646.3 cm <sup>-1</sup> 1652.1 cm <sup>-1</sup> 1659.3 cm <sup>-1</sup> 1669.1 cm <sup>-1</sup> 1678.1 cm <sup>-1</sup>	$\beta$ -sheet (70.9%) $\beta$ -sheet (4.3%) $\beta$ -sheet (7.9%) $\beta$ -sheet (1.0%) random coils (2.8 %) $\alpha$ -helical (0.7%) $\alpha$ -helical (4.3%) $\beta$ -turns (2.9%) $\beta$ -turns (5.3%)
6.	Freeze-thaw	1643 cm <sup>-1</sup>	1602.2 cm <sup>-1</sup> 1631.7 cm <sup>-1</sup> 1656.2 cm <sup>-1</sup> 1659.8 cm <sup>-1</sup>	$\beta$ -turns (15.5%) $\beta$ -sheet (29.5%) $\alpha$ -helical (8.7%) $\alpha$ -helical (46.3%)

Furthermore, the 1100-1000 cm<sup>-1</sup> spectral interval was also analyzed/ deconvoluted in native as well as decellularized corneas as the peaks appearing in this region are attributed to the C-OH stretching vibrations of carbohydrate moieties present in the proteoglycans of corneal matrix.<sup>29</sup>

In the case of untreated cornea, various peaks were obtained in 1100-1000  $\text{cm}^{-1}$  spectral interval (**Fig. 4 a2**) at 1030.2  $\text{cm}^{-1}$ , 1043.5  $\text{cm}^{-1}$ , 1052.3  $\text{cm}^{-1}$ , 1061.2  $\text{cm}^{-1}$ , 1073.4  $\text{cm}^{-1}$  and 1088.3  $\text{cm}^{-1}$ . In the case of direct perfused cornea with 0.1% TRITON, peaks appeared at 1029.2  $\text{cm}^{-1}$ , 1043.2  $\text{cm}^{-1}$ , 1054.1  $\text{cm}^{-1}$ , 1060.3  $\text{cm}^{-1}$ , 1074.5  $\text{cm}^{-1}$  and 1087.3  $\text{cm}^{-1}$  (**Fig. 4 b2**). In liquid nitrogen treated cornea (**Fig. 4 c2**), peaks were visible at 1009.2  $\text{cm}^{-1}$ , 1024.9  $\text{cm}^{-1}$ , 1038.9  $\text{cm}^{-1}$ , 1060.3  $\text{cm}^{-1}$ , 1082.4  $\text{cm}^{-1}$  and 1091.9  $\text{cm}^{-1}$ . In the case of TRITON (0.5%, orbital shaker), peak appeared at 1029.3  $\text{cm}^{-1}$  and 1074.5  $\text{cm}^{-1}$ . (**Fig. 4 d2**), while in SDS (0.1%, orbital shaker) treated cornea (**Fig. 4 e2**), these were present at 1000.2  $\text{cm}^{-1}$ , 1022.9  $\text{cm}^{-1}$ , 1033.2  $\text{cm}^{-1}$ , 1056.3  $\text{cm}^{-1}$  and 1075.4  $\text{cm}^{-1}$ . In freeze thaw treated cornea (**Fig. 4 f2**), this peak appeared at 1027.3  $\text{cm}^{-1}$ , 1058.4  $\text{cm}^{-1}$  and 1076.7  $\text{cm}^{-1}$ .

Various peaks were obtained in 1000-1100  $\text{cm}^{-1}$  range in each of the decellularized cornea and also, native cornea. However, spectral peak due to C-O stretching vibration which is specific for keratan sulphate (GAG) appeared at 1043  $\text{cm}^{-1}$ , in native and perused corneas only.<sup>33</sup> Thus the result indicated relatively high GAG content in perfused cornea as compared to other decellularized cornea.

**Table 4.** Deconvoluted spectral peaks in 1100-1000  $\text{cm}^{-1}$  interval.

Sr. No.	Tissue	Peak positions	Deconvoluted peaks
1.	Native	1075 $\text{cm}^{-1}$	1030.2 $\text{cm}^{-1}$ , 1043.5 $\text{cm}^{-1}$ , 1052.3 $\text{cm}^{-1}$ , 1061.2 $\text{cm}^{-1}$ , 1073.4 $\text{cm}^{-1}$ , 1088.3 $\text{cm}^{-1}$
2.	TRITON, 0.1% (Direct perfusion)	1074 $\text{cm}^{-1}$	1029.2 $\text{cm}^{-1}$ , 1043.2 $\text{cm}^{-1}$ , 1054.1 $\text{cm}^{-1}$ , 1060.3 $\text{cm}^{-1}$ , 1074.5 $\text{cm}^{-1}$ ,



			1087.3 cm <sup>-1</sup>
3.	Liquid Nitrogen	1068 cm <sup>-1</sup>	1009.2 cm <sup>-1</sup> , 1024.9 cm <sup>-1</sup> , 1038.9 cm <sup>-1</sup> , 1060.3 cm <sup>-1</sup> , 1082.4 cm <sup>-1</sup> 1091.9 cm <sup>-1</sup> .
4.	TRITON (0.5%, orbital shaker)	1069 cm <sup>-1</sup>	1029.3 cm <sup>-1</sup> , 1074.5 cm <sup>-1</sup>
5.	SDS (0.1%, orbital shaker)	1070 cm <sup>-1</sup>	1000.2 cm <sup>-1</sup> , 1022.9 cm <sup>-1</sup> , 1033.2 cm <sup>-1</sup> , 1056.3 cm <sup>-1</sup> , 1075.4 cm <sup>-1</sup>
6.	Freeze-thaw	1070 cm <sup>-1</sup>	1027.3 cm <sup>-1</sup> , 1058.4 cm <sup>-1</sup> , 1076.7 cm <sup>-1</sup>

### 3.4 Raman spectroscopic study

Amide I peaks appeared at 1673 cm<sup>-1</sup> and 1668 cm<sup>-1</sup> which represents Col IV and Col I respectively (**Fig. 5**).<sup>30</sup> Native cornea and perfused cornea exhibited peaks at 1673 cm<sup>-1</sup> and 1672 cm<sup>-1</sup> respectively due to amide I band vibration. This peak appeared at 1671 cm<sup>-1</sup> in liquid nitrogen, TRITON (0.5%, orbital shaker) and SDS (0.1%, orbital shaker) treated corneas while around 1680 cm<sup>-1</sup> in freeze thaw treated cornea. Thus appearance of amide I peak around 1673 cm<sup>-1</sup> in most of the decellularized cornea might indicate presence of Col IV found in Descemet's membrane of the corneal tissue.<sup>31</sup> Shift of amide I peak to higher wave numbers in freeze thaw treated cornea could be due to deformation of collagen fibres. Furthermore, variation in peak intensity can be correlated to preservation of Descemet's membrane. Peak intensity of amide I band was found highest in perfused cornea indicating intact Descemet's membrane of the cornea tissue. In native cornea, along with one major peak of amide I, one shoulder peak appeared at

around  $1614\text{ cm}^{-1}$  that corresponds to  $\beta$ -turns or aggregates present in native corneal tissue. The intensity of this peak was found very low in other decellularized corneas; 0.46, 0.19 and 0.39 fold decrease was observed in liquid nitrogen, SDS (0.1%, orbital shaker) and TRITON (0.5%, orbital shaker) respectively. Decrease in intensity might indicate loss of this membrane during decellularization process.

Collagen secondary structural differences between native and differently decellularized cornea can be assessed by Amide III band analysis. Amide III major peak at  $1271\text{ cm}^{-1}$  attributes to proline poor (polar) region of the collagens. Peak around  $1271\text{ cm}^{-1}$  indicates  $\alpha$ -helical structure of the collagen fibres while  $1247\text{ cm}^{-1}$  indicates random coil structure of collagen fibres.<sup>30</sup> A peak at around  $1273\text{ cm}^{-1}$  appeared in perfused cornea which indicates  $\alpha$ -helical structure. In liquid nitrogen, SDS (0.1%, orbital shaker) and TRITON (0.5%, orbital shaker) treated cornea this peak was shifted towards 1277, 1283 and  $1278\text{ cm}^{-1}$  respectively. Shift of this peak to higher wavenumber indicates disruption of collagen  $\alpha$ -helical structure to  $\beta$ -sheets.

In native cornea peaks appeared at 817 and  $939\text{ cm}^{-1}$  corresponding to vibrational modes of protein backbone.<sup>33</sup> In directly perfused cornea, these peaks appeared at 817 and  $941\text{ cm}^{-1}$ . In liquid nitrogen treated cornea, peaks were observed at 820 and  $940\text{ cm}^{-1}$  thus  $817\text{ cm}^{-1}$  peak shifts up by  $3\text{ cm}^{-1}$ . In SDS (0.1%, orbital shaker) and TRITON (0.5%, orbital shaker) peak positions were found similar to native cornea. In freeze thaw treated cornea, peak corresponding to  $817\text{ cm}^{-1}$  was missing while peak of  $939\text{ cm}^{-1}$  shifted to  $945\text{ cm}^{-1}$  that indicates disruption of protein ultrastructure.

Keratan sulphate, the main GAG component of proteoglycans present in the corneal tissue,<sup>34</sup> consists of C-O<sup>-</sup> and OSO<sub>3</sub><sup>-</sup> groups that vibrate to give specific spectral peaks in ATR-FTIR and Raman spectroscopic studies which can be used to observe the difference in GAG content of differently decellularized cornea. In this study, spectral peaks due to C-O<sup>-</sup> stretching vibration mainly observed in ATR-FTIR only while peak around 1000 cm<sup>-1</sup> correspond to OSO<sub>3</sub><sup>-</sup> equatorial position appeared in Raman spectra.<sup>35</sup> Furthermore, bands appearing around 1000 and 1033 cm<sup>-1</sup> correspond to phenylalanine residues that also indicate presence of collagen type IV.<sup>36</sup> High peak intensity was observed in perfused cornea while it was found very less in SDS (0.1%, orbital shaker) and freeze thaw treated cornea with 0.103 and 0.038 fold decreases in intensity as compare to directly perfused cornea. This indicated preservation of GAG content in perfused cornea.

Taken together, corneal decellularization by direct perfusion of TRITON (0.1%) was more suitable compared to the other methods as it completely stripped the cells off the matrix while still preserving the ultrastructural organization of ECM. This was also evident from the peak intensities observed as a result of different treatment methods. This decrease in intensity has previously been reported to be directly related to the stretching of collagen fibres.<sup>33</sup>

### 3.5. FACS Analysis

Under different processing conditions, cell death may occur disproportionately as a portion of the cells undergo either necrosis or apoptosis. FACS was done to determine the percentage of corneal cells undergoing apoptotic cell death over necrotic cell death

during decellularization. Apoptotic cells appeared to be annexin V positive and PI negative, whereas necrotic cells were annexin V negative and PI positive. Undamaged cells remained negative for both annexin V and PI staining. In untreated cornea, a high percentage (71%) of cells was scored viable by the absence of annexin V-binding and PI uptake (lower left quadrant) (**Fig. 6a**). The early apoptotic cells showed an intact cytoplasmic membrane, with the absence of PI staining (**Fig. 6 a2**). This subpopulation corresponded to 26.5% of the total cells. While late apoptotic cells depicted positive staining for both annexin V and PI staining (**Fig. 6 a1**). Liquid nitrogen (**Fig. 6b**) and freeze thaw (**Fig. 6c**) treated corneas showed comparable results comprising of 45.2% and 50.6% of cells in the early apoptotic phase. There was a remarkable difference in the apoptotic cell population between direct perfused (**Fig. 6d**) and orbital shaker (**Fig. 6e**) treated cornea as apoptosis was predominant in the former, possessing 13.1% higher apoptotic cells than the later.

### 3.6. Analysis of the optical properties of the decellularized tissue

Visible differences in the gross transparency levels of decellularized corneal tissues were evident with varied with respect to the decellularization protocol (**Fig. 7A**). Upon visual examination, the liquid nitrogen treated cornea appeared to be the most lucid (**Fig. 7A**). Moreover, the transmittance was quantified by spectrophotometry (**Fig. 7B**). The highest value of light transmittance was observed in liquid nitrogen treated cornea (40% transmittance at 400 nm and 60% transmittance at 800 nm) over untreated cornea (60% transmittance at 400 nm and 87% transmittance at 800 nm). Direct perfused corneas were able to transmit 35% light at 400 nm and 50% light at 800 nm; these values are found to be higher than orbital shaker treated cornea (**Fig. 7B**). Though liquid

nitrogen treated cornea displayed higher transmittance amongst all the decellularization processes, it could be due to the presence of intact endothelium,<sup>7</sup> however incomplete removal of cells, as demonstrated by H&E staining (**Fig. 2**) makes this strategy less suitable.

### 3.7 Fibre orientation analysis

The coherencycoherency coefficient for the decellularized corneas was evaluated by orientationJ (**Table 5, Fig. S2**). Of all the treatment methods used, only the values for direct perfused cornea (10  $\mu$ l/min) and for native cornea were found to be in similar range corresponding to  $0.363 \pm 0.04$  and  $0.27 \pm 0.04$  respectively. This indicated that the fibre distribution of perfusion treated corneal matrix resembled to that of native cornea, whereas more dispersive orientation of collagen fibers was observed in other decellularization protocols with coherencycoherency coefficient values of  $<0.01$ .

**Table 5:** Coherence coefficient of decellularized corneas treated by different methods.

Decellularization method	Native Cornea	Direct Perfusion	TRITON (Orbital shaker, 0.5%)	SDS (Orbital shaker, 0.1%)	Freeze-thaw	Liquid Nitrogen
Coherence coefficient	$0.27 \pm 0.04$	$0.363 \pm 0.04$	$0.018 \pm 0.002$	$0.034 \pm 0.005$	$0.012 \pm 0.022$	$0.022 \pm 0.04$

### 3.8 Recellularization

The decellularized cornea obtained using TRITON (0.1%)-direct perfusion method was selected as the candidate matrix for recellularization studies owing to its

intact ultrastructure, resembling native corneal tissue (**Fig. 8 A and B**). After 7 days in culture, H&E (**Fig. 8C**) and DAPI (**Fig. 8D**) staining revealed that the goat keratocytes appeared well attached and uniformly distributed throughout the matrix exhibiting typical spindle shaped cellular morphology clearly aligned along the direction of the ECM fibrils with more or less intact cell membrane integrity. Furthermore, quantitative analysis revealed extensive coverage of the porous recellularized cornea with keratocytes which was significantly higher on decellularized matrix ( $87 \pm 19.7$  cells per field) as compared to native cornea ( $36 \pm 25.35$  cells per field), possibly due to the porous architecture of the decellularized matrix.

## Discussion

In our study, direct perfusion of detergent emerged as a highly efficient protocol for decellularization of corneal tissue. Though perfusion based decellularization has successfully been attempted for complex organs like kidney<sup>28</sup> and heart,<sup>5</sup> the studies utilized a high throughput system for perfusing the detergents, chemically and mechanically, over the whole tissue or through the vasculature to circulate the fluid within the respective tissues. On the other hand, in our study, we used a perfusion chamber for placing the corneas precisely in the centre to facilitate direct perfusion of the decellularizing agents throughout the cornea. We believe that since this system allows perfusion of the decellularizing agents directly through the tissues (rather than perfusion around or through blood vessels), it would allow uniform and affective removal of the resident cell population.

All conventional approaches for tissue decellularization induce cell lysis. In cases where the resultant cell debris re-attaches itself to the decellularized matrix, an extensive immunogenic reaction can be triggered.<sup>11</sup> Moreover, most methods employed have led to the disruption of the matrix or its constitutional components thus rendering a partially functional deactivity.<sup>13</sup> Therefore for successful decellularization to occur, the tissues should fulfill the following essential criteria; (1) DNA content should be equal to or less than 50 ng/mg of tissue with residual DNA fragments below 200 bp in length, (2) histochemical data should show no visible evidence of cellular and DNA fragments, (3) native ECM of the decellularized tissue should be preserved.<sup>28</sup> The remarkable finding accomplished in this study was that complete removal of cells with minimal disturbance in the Descemet's membrane and Bowman's membrane, resembling native cornea, with intact ultrastructure was attained with a non-ionic detergent, TRITON, at a mere concentration of 0.1% at a flow rate of 10  $\mu$ l/min (**Fig. 8 A and B**). This contradicts all the reported findings which suggest that the use of only harsh ionic detergents such as SDS could fulfill the decellularization criteria.<sup>5,6</sup>

In the present study, we evaluated a total of four methods (including physical and chemical methods) to test their effectiveness in cellular removal from the corneal tissue while preserving the ECM ultrastructure. Among the physical methods employed, incubating corneas in liquid nitrogen has reportedly induced cell apoptosis, as only freezing may not be sufficient for complete decellularization.<sup>16</sup> However, liquid nitrogen treatment is considered as a relatively mild treatment over detergent based methods and therefore often needs to be supplemented with extensive washing of the tissue under hydrostatic pressure<sup>15</sup> to ensure complete removal of residual cells which renders it less

convenient in context of clinical application. Furthermore, SDS (0.1%, 0.5%) in orbital shaker showed no visible evidence of cellular or nuclear material (**Fig. 2**) and also the measured DNA content level was below 50 ng/mg tissue (**Fig. 3**), which qualifies it as a suitable detergent for decellularization protocols. This result was consistent with the findings of Sullivan et al,<sup>28</sup> where 0.5% SDS was found to completely decellularize the porcine kidneys when compared with three different detergent concentrations; 0.25% SDS, 0.5% SDS and 1% TRITON by high throughput perfusion based system. When used in lower concentrations upto 0.1% SDS, cellular remnants [about 18 keratocytes/field of view (0.08 mm<sup>2</sup> area)] were found in the decellularized tissue.<sup>37</sup> While contradictory studies which have also demonstrated that isotonic buffer of 0.1% SDS for 7 h can completely decellularize cornea with minimum structural disruption.<sup>38</sup> However, even in such low concentrations, SDS has proven to have deleterious effects on the ECM ultrastructure as also observed in our study.<sup>18</sup> Further to this, spectroscopy data (ATR-FTIR and Raman spectroscopy) supported the fact that SDS (0.1%) rendered adverse effects on collagen conformation (**Fig. 4 and 5**) and was therefore considered unsuitable for decellularization of corneas. Moreover, a reduction in the transparency of the decellularized cornea was also observed with SDS (**Fig. 6**). This phenomenon, previously seen by other groups<sup>18</sup> is usually restored by immersing the tissues in glycerol.<sup>12</sup>

On the other hand, TRITON (at 0.1%, 0.5%) in orbital shaker, could not entirely remove the cellular material from goat cornea (**Fig. 2**) primarily due to its mild nature.<sup>39</sup> Still others have reported the use of TRITON for corneal decellularization at concentrations as low as 0.2%, which when implanted in lamellar keratoplasty of rabbit models provoked no adverse reactions. However, TRITON alone was insufficient and



therefore used in combination with either mild salt solution (2M NaCl)<sup>17</sup> or hydroxylamine<sup>39</sup> to ensure complete removal of cells and debris. Whereas, in higher concentrations of up to 2% combined with gentle shaking, TRITON has been reported to effectively decellularize the native cells from corneal stroma within 72 h while preserving the ECM architecture, as verified by the presence of Col I, II, III, IV and fibronectin.<sup>7</sup> While application of such high concentrations of detergent solution can successfully remove the cellular material, they are often associated with aggregation of proteins which ultimately lead to ECM damage.<sup>11</sup> This was confirmed by Shafiq and co-workers when they could no longer detect laminin; important cellular matrix adhesion protein present in ECM for attachment of corneal epithelial cells, in the epithelial basement membrane of decellularized human corneas after treatment with 2% TRITON.<sup>39</sup> The fact that with direct perfusion, TRITON at a mere 0.1% concentration lead to complete cellular removal with the preservation of native collagen fibril architecture and retention of the non fibrillar component (proteoglycan), as determined by spectroscopy by studying the secondary structure of constituent proteins<sup>41</sup> proves the superiority of the method.

Apart from the concentration of the detergent used, the perfusion flow rate was also found to have a profound effect on the extent of decellularization of corneal stroma and ECM organization (**Fig. S1**). Previous literature has shown that automated perfusion systems performed on lung tissue for decellularization required a mixture of different detergents (0.1% TRITON, 2% SDS) and enzymatic solutions (DNase) to completely decellularize the tissue<sup>39</sup> at high (0.6 ml/min) perfusion speeds.<sup>40</sup> However, using the direct perfusion based chamber we were able to achieve complete cellular removal at extremely lower flow rates. Minimal disruption of the native architecture of collagen was

observed at 10  $\mu$ l/min, below which there was incomplete removal of cells (data not shown). The deleterious effects of higher flow rates (>10  $\mu$ l/min) were evident from the partial disruption of Descemet's membrane observed at 50  $\mu$ l/min perfusion (**Fig. S1 A**) and complete disruption of the membrane at 100  $\mu$ l/min (**Fig. S1 B**). This may be due to the continuous unidirectional perfusion with detergent followed by PBS which might loosen the cells within the stromal matrix ultimately generating forces to plunge the cells out of the tissue. When this expulsive force exceeds the threshold, it leads to extensive tissue damage. Moreover, at the optimum flow rate of 10  $\mu$ l/min used, the perfusion pressure generated during the fluid flow predominates over the cell lysis caused by the detergent, as supported by flow cytometric evidence (**Fig. 6**). Therefore, the proposed direct perfusion system does not entirely rely on cell lysis by the detergent, but also on the perfusion pressure and flow regime. Thus, this stress stimulus might be responsible for the triggering of apoptotic cell death<sup>42</sup> or the resident corneal cells may follow a p53 independent apoptotic pathway.<sup>43</sup> The detailed mechanism of cell death during decellularization needs to be probed further.

A strikingly different pattern of cell death has been observed in perfusion and orbital shaker methods from the FACS histogram (**Fig. 6**). A significantly higher percentage of cells (13%) underwent apoptotic cell death in direct perfusion (**Fig. 6d**) over orbital shaker method (**Fig. 6e**), which reinforces the concept that direct perfusion generates a mild force on the tissue and the unidirectional fluid flow assists in the removal of cells as well as coaxes the cells down the apoptosis path. The induction of apoptosis in the corneal cells during tissue decellularization, as observed in the perfusion method, is the preferred pathway of cell death as compared to necrosis.<sup>11</sup> This is due to

the fact that early loss in membrane integrity during necrosis results in massive inflammation reactions, while apoptosis leads to phagocytosis by immune cells, thereby suppressing the immune reactions.<sup>44</sup> However, future studies should also focus on determining the immunogenicity of such decellularized xenografts to ensure their extended survival rates post implantation. It is known that cornea is an immune-privileged tissue is therefore not very prone to rejection like most other organs, provided cornea is efficiently decellularized *via* the apoptotic pathway. However, the leakage of contents within the surrounding matrix which is common occurrence in the necrosis pathway may not only provoke extensive immune infiltration, but can also act as a carrier of infectious disease transfer between the two species.<sup>37</sup> Another additional advantage of apoptosis in ECM decellularization is associated with the intimate relationship between the effector caspases<sup>44</sup> and Prostaglandin E2 (PGE2),<sup>45</sup> whereby the activation of the former regulates the release of the latter. This process has reportedly influenced tissue regeneration *via* induction of proliferation in progenitor cells located within the niche. Hence conditioning the matrix for tissue decellularization *via* apoptotic pathway seems to be regulated by the release of some important paracrine signals. Hence decellularizing a tissue through the apoptotic pathway may contribute to remodel the matrix towards regeneration programs by releasing key paracrine signals.<sup>11</sup> Slow perfusion of detergent through cornea tissue was found to trigger apoptotic pathway, meeting the opinion made by Bourguine *et al* that complete decellularization with integrated ECM could be achieved by triggering apoptotic pathway in combination of perfusion system.<sup>11</sup> However, a major shortcoming in the present study was that we were not able to distinguish between the early and late stages of apoptosis. According to a recent study by Bauchle and co-

workers, Raman spectrophotometry could be successfully employed to identify the stages of cell modalities, including apoptosis (both early and late) and necrosis. However, the method needs to be applied directly on the cells prior to decellularization of the tissue.<sup>46</sup>

To the best of our knowledge, this is the first study to demonstrate the use of spectroscopic tools including ATR-FTIR and Raman spectroscopy for characterizing decellularized corneal matrices. Decellularized ECM composed predominantly of stromal region that is rich in Col I and comprised of more than 75% of total corneal collagens.<sup>47</sup> In ATR-FTIR analysis, amide-I band region was used to demonstrate the overall changes that occurred post-treatment in the secondary structure of collagen<sup>36</sup> in decellularized cornea (**Fig. 4**). It was revealed that all decellularization methods resulted in certain degree of alteration in amide-I band (CO). However, the spectra obtained after TRITON (0.1%) treatment in direct perfusion system yielded peaks due to the presence of random coils ( $1646\text{ cm}^{-1}$ ) and  $\alpha$ -helical ( $1655\text{ cm}^{-1}$ ) structures (**Fig. 4**) typically observed in untreated corneas indicating no disturbance in the collagen secondary structure (**Fig. 4 and 5**), hence confirming its efficacy over other methods. Whereas only one peak corresponding to the triple helical secondary structure of collagen was obtained ( $1636\text{ cm}^{-1}$ ) in the case of SDS (0.5%) in orbital shaker. Detergents tend to interact with collagen, first on the basis of electrostatic forces, followed by a combination of electrostatic forces and hydrophobic reactions, which are more pronounced in ionic detergents as compared to non ionic detergents like TRITON.<sup>47</sup> Such strong interactions often result in the denaturation of proteins, as observed in the case of SDS.

As expected, this decellularized corneal matrix obtained after direct perfusion of detergent was found to support the corneal stromal cell culture for 7 days in dynamic

condition, as reports have shown that dynamic condition is required for sufficient infiltration of nutrients and oxygen for the dense tissue like cornea.<sup>14</sup> Freeze drying method was employed to develop the matrix as it preserves the ECM components by arresting chemical and biological reactions in frozen state. Our finding is promising as many previously reported studies<sup>48</sup> failed to demonstrate infiltration of keratocytes into the decellularized cornea as the resultant matrix post-decellularization treatment was bioinert and therefore could not support the cell-ECM attachment. The relatively higher recellularization efficiency in decellularized matrix compared to native cornea could be due to the higher cell number used or porous structure of the matrix, a prerequisite for recellularization.<sup>14</sup> Thus perfusion based strategy has the potential to give an efficient, complete and closed system for decellularization, cellular isolation and reseeding the acellular matrix.

Prior to clinical trials, future studies in xeno-graft transplantation models will focus on evaluating whether the genetic difference between the cadaveric donor, goat, and recipient human, elicits any type of immunogenic response to the matrix which may ultimately lead to implant rejection; inspite of the immune-privileged nature of cornea. This phenomenon occurs by binding of anti-Gal antibodies to the  $\alpha$ -gal epitope on proteoglycans and glycoproteins of decellularized ECM. If a positive reaction occurs between the antibody and the ECM, this may trigger matrix degradation by accelerating macrophage-mediated immune response. In this regard, another important consideration is whether perfusion based decellularized corneal matrix hold any advantage over other conventional techniques in terms of reducing the immunogenicity of the resultant graft.

Beyond the corneal reconstruction potential, this new matrix can be used as *in vitro* model system to generate insights about corneal development or pathological conditions.

## 5. Conclusion

This study postulates an efficient and relatively simple protocol for corneal decellularization by direct perfusion of a mild non-ionic detergent TRITON at low concentration. Direct perfused matrix characterized for complete decellularization along with preservation of the precise collagen architecture and ECM milieu. An important feature of direct perfusion technique was that the procedure resulted in a greater number of the resident corneal cells undergoing apoptosis instead of necrosis, which may lead to a subdued immune response. These findings suggested that the direct perfusion of corneal tissue was able to generate optimal decellularized matrix for tissue engineering and transplantation purposes.

**Acknowledgement:** This study was funded by intramural funding from IIT Delhi (High Impact project) and funding from Department of Biotechnology (BT/PR5717/MED/32/244/2012). Authors are grateful to SMITA laboratory of IIT Delhi for providing access to Confocal laser dispersion Micro-Raman spectrometer.

## Figure Legends

**Fig. 1** Schematic representation of the four different methods used for the decellularization of goat cornea.

**Fig. 2** Histological analysis of decellularized cornea to compare the efficiency of the various cell removal techniques. Left panel: Light micrographs of H&E (Scale 200  $\mu\text{m}$ ); Centre: Higher magnification H&E (Scale 50  $\mu\text{m}$ ); Right panel: Fluorescence images of DAPI (Scale 50  $\mu\text{m}$ ). Top to bottom: **Physical methods**; (a1-a3): liquid nitrogen, (b1-b3): freeze-thaw, **Chemical methods**; (c1-c3): 0.1% SDS in orbital shaker, (d1-d3): 0.5% SDS in orbital shaker, (e1-e3): 0.1% TRITON in orbital shaker, (f1-f3): 0.5% TRITON in orbital shaker, **TRITON in perfusion chamber at different flow rates**; (g1-g3): 10  $\mu\text{l/min}$ , (h1-h3): 50  $\mu\text{l/min}$ , (i1-i3): 100  $\mu\text{l/min}$ .

**Fig. 3** Biochemical analysis of decellularized cornea; (A) GAG content and (B) total DNA content (\*  $p < 0.01$ ,  $n = 3$ ). GAG analysis revealed that TRITON, 0.1% (Direct Perfusion) is most efficient in preserving the ECM content of the corneas. For DNA analysis, both SDS 0.1% (OS) and TRITON, 0.1% (Direct Perfusion) methods gave satisfactory results compared to other methods. Hence TRITON, 0.1% (Direct Perfusion) method decellularized cornea as well as preserved the native extracellular matrix components of the corneal tissue. Abbreviation: ECM-Extracellular matrix, OS - Orbital shaker.

**Fig. 4** (a) ATR-FTIR of decellularized and native corneas. Deconvoluted spectra of 1600-1700  $\text{cm}^{-1}$  spectral interval, (b1) Native cornea; (b2) TRITON, 0.1% (Direct Perfusion); (b3) Liq. Nit.; (b4) Freeze Thaw; (b5); (b6) TRITON (0.5%), (OS). Deconvoluted spectra

of 1000-1100  $\text{cm}^{-1}$  spectral interval, (c1) Native cornea, (c2) TRITON, 0.1% (Direct Perfusion), (c3) Liq. Nit., (c4) Freeze Thaw, (c5) SDS, 0.1% (OS), (c6) TRITON (0.5%) (OS). Abbreviation: Liq. Nit - Liquid Nitrogen.

**Fig. 5** Raman spectra of decellularized corneas excited at 488 nm. The Amide I (1600-1700  $\text{cm}^{-1}$ ), Amide III (1200-1300  $\text{cm}^{-1}$ ), GAG (1000-1100  $\text{cm}^{-1}$ ) and Protein backbone (800-900  $\text{cm}^{-1}$ ) regions are zoomed in the insets to show the corresponding peaks elucidating the corneal chemistry.

**Fig. 6** FACS scatterplots of stromal cells isolated from decellularized cornea processed by different methods and stained with annexin V (green) and propidium iodide (red); (a) Native, (b) Liq. Nit., (c) Freeze Thaw, (d) TRITON, 0.1% (Direct Perfusion), (e) TRITON, 0.1% (OS). Representative fluorescent images (scale 10  $\mu\text{m}$ ) of (a1) necrotic cells, (a2) apoptotic cells.

**Fig. 7 (A)** Transparency of cornea; (a1) untreated, (a2) treated with liquid nitrogen, (a3) TRITON (0.1%)-direct perfusion, (a4) TRITON (0.5%)-Orbital shaker, (a5) freeze-thaw and (a6) SDS (0.1%)-Orbital shaker. **(B)** Transmittance measurements of decellularized cornea using different methods.

**Fig. 8** H&E staining: A; Native cornea displaying intact Bowman's (a1) and Descemet's membrane (a2), B; Decellularized cornea with TRITON (0.1%)- direct perfusion at 10  $\mu\text{l}/\text{min}$  with intact Bowman's (b1) and Descemet's membrane (b2), C; Cells uniformly dispersed into the matrix after recellularization and DAPI staining (D) of recellularized corneal matrix obtained from direct perfusion showing the presence of goat keratocytes seeded on decellularized corneal matrices.



## References

1. M.O. Price and F.W. Price, *Current Opinion in Ophthalmology*, 2007, **18**, 290-294.
2. P. Fagerholm, N.S. Lagali, K. Merrett, W.B. Jackson, R. Munger, Y. Liu, J. W. Polarek, M. Söderqvist and M.A. Griffith, *Sci. Transl. Med.*, 2010, **2**, 46-61.
3. H. Hara and D. K. Cooper, *Cornea*, 2011, **30**, 371-378.
4. A. P. Price, K. A. England, A. M. Matson, B. R. Blazar and A. Panoskaltsis-Mortari, *Tissue Eng Part A*, 2010, **16**, 2581-2591.
5. H.C. Ott, T.S. Matthiesen, S.K. Goh, L.D. Black, S.M. Kren, T.I. Netoff and D.A. Taylor, *Nature Medicine*, 2008, **14**, 213-221.
6. T. Shupe, M. Williams, A. Brown, B. Willenberg and B. E. Petersen, *Organogenesis*, 2010, **6**, 134-136.
7. J. S. Choi, J. K. Williams, M. Greven, K. A. Walter, P. W. Laber, G. Khang and S. Soker, *Biomaterials*, 2010, **31**, 6738-6745.
8. K. Musselmann, B. Kane, B. Alexandrou and J. R. Hassell, *Invest Ophthalmol Vis Sci*, 2006, **47**, 5260-5266.
9. K.M. Meek and C. Boote, *Experimental Eye Research*, 2004, **78**, 503–512.
10. L.W. Samantha, E.S. Laura, E.D. Siobhán, B.R. James and H. Andrew, *J. Funct. Biomater.*, 2013, **4**, 114–161.
11. P. E. Bourguine, B. E. Pippenger, A. Todorov, L. Tchang and I. Martin, *Biomaterials*, 2013, **34**, 6099-6108.
12. K. Pang, L. Du and X. Wu, *Biomaterials*, 2010, **31**, 7257-7265.
13. P. Vavken, S. Joshi and M. M. Murray, *J Orthop Res*, 2009, **27**, 1612-1618.

14. J. Xiao, H. Duan, Z. Liu, Z. Wu, Y. Lan, W. Zhang, C. Li, F. Chen, Q. Zhou, X. Wang, J. Huang and Z. Wang, *Biomaterials*, 2011, **32**, 6962-6971.
15. Y. Hashimoto, S. Funamoto, S. Sasaki, T. Honda, S. Hattori, K. Nam, T. Kimura, M. Mochizuki, T. Fujisato, H. Kobayashi and A. Kishida, *Biomaterials*, 2010, **31**, 3941-3948.
16. S. Amano, N. Shimomura, S. Yokoo, K. Araki-Sasaki and S. Yamagami, *Mol Vis*, 2008, **14**, 878-882.
17. H. Luo, Y. Lu, T. Wu, M. Zhang, Y. Zhang and Y. Jin, *Biomaterials*, 2013, **34**, 6748-6759.
18. M. Gonzalez-Andrades, J. de la Cruz Cardona, A. M. Ionescu, A. Campos, M. Del Mar Perez and M. Alaminos, *Invest Ophthalmol Vis Sci*, 2011, **52**, 215-222.
19. C. Zhang, X. Nie, D. Hu, Y. Liu, Z. Deng, R. Dong, Y. Zhang and Y. Jin, *Cell Tissue Res*, 2007, **329**, 249-257.
20. S. Roy, P. Silacci and N. Stergiopulos, *Am J Physiol Heart Circ Physiol*, 2005, **289**, H1567-1576.
21. A. Scherberich, R. Galli, C. Jaquier, J. Farhadi and I. Martin, *Stem Cells*, 2007, **25**, 1823-1829.
22. Y. Martin and P. Vermette, *Biomaterials*, 2005, **26**, 7481-7503.
23. S.Y. Proskuryakov, A.G. Konoplyannikov and V.L. Gabai, *Exp Cell Res*, 2003, **283**, 1-16.
24. A. Podskochoy, L. Gan and P. Fagerholm, *Cornea*, 2000, **19**, 99-103.
25. L. Wang, T. Li and L. Lu, *Invest Ophthalmol Vis Sci*, 2003, **44**, 5095-5101.
26. H. Bakhshandeh, M. Soleimani, S. S. Hosseini, H. Hashemi, I. Shabani, A. Shafiee,

- A. H. Nejad, M. Erfan, R. Dinarvand and F. Atyabi, *Int J Nanomedicine*, 2011, **6**, 1509-1515.
27. M. Bhattacharjee, S. Chameettachal, S. Pahwa, A. R. Ray and S. Ghosh, *ACS Appl Mater Interfaces*, 2014, **6**, 183-193.
28. D. C. Sullivan, S. H. Mirmalek-Sani, D. B. Deegan, P. M. Baptista, T. Aboushwareb, A. Atala and J. J. Yoo, *Biomaterials*, 2012, **33**, 7756-7764.
29. C. Petibois, G. Gouspillou, K. Wehbe, J. P. Delage and G. Dél  ris, *Anal Bioanal Chem*, 2006, **386**, 1961-1966.
30. T.T. Nguyen, C. Gobinet, J. Feru, S. Brassart-Pasco, M. Manfait and O. Piot, *Spectroscopy: An International Journal*, 2012, **27**, 421-427.
31. J.M. Fitch, D.E. Birk, C. Linsenmayer and T.E. Linsenmayer, *Journal of Cell Biology*, 1990, **110**, 1457-1468.
32. M. Ga  sior-G  logowska, M. Komorowska, J. Hanuza, M. Ptak and M. Kobi  larz, *Acta Bioeng Biomech*, 2010, **12**, 55-62.
33. A. J. Quantock, R. D. Young and T. O. Akama, *Cell Mol Life Sci*, 2010, **67**, 891-906.
34. N. Mainreck, S. Br  zillon, G. D. Sockalingum, F. X. Maquart, M. Manfait and Y. Wegrowski, *J Pharm Sci*, 2011, **100**, 441-450.
35. C. Gullekson, L. Lucas, K. Hewitt and L. Kreplak, *Biophys J*, 2011, **100**, 1837-1845.
36. W. Lee, Y. Miyagawa, C. Long, D. K. Cooper and H. Hara, *Int J Ophthalmol*, 2014, **7**, 587-593.
37. Z. Yang, W. Zheng, G. Jian, W. Pengxia, L. Naiyang, X. Peng, G. Qianying and Z. Wang, *Cornea*, 2011, **30**, 73-82.

38. M. A. Shafiq, R. A. Gemeinhart, B. Y. Yue and A. R. Djalilian, *Tissue Eng Part C Methods*, 2012, **18**, 340-348.
39. A. P. Price, L. M. Godin, A. Domek, T. Cotter, J. D'Cunha, D. A. Taylor and A. Panoskaltsis-Mortari, *Tissue Eng Part C Methods*, 2015, **21**, 94-103.
40. S. Wang, H. Oldenhof, A. Hilfiker, M. Harder and W.F. Wolkers, *Biomed. Spectrosc. Imaging*, 2012, **1**, 79–87.
41. S. Oh, Y. Kim, J. Kim, D. Kwon and E. Lee, *Biochemical and Biophysical Research Communications*, 2010, **399**, 91–97.
42. H. Erdal, M. Berndtsson, J. Castro, U. Brunk, M. C. Shoshan and S. Linder, *Proc Natl Acad Sci U S A*, 2005, **102**, 192-197.
43. W. Strupp, G. Weidinger, C. Scheller, R. Ehret, H. Ohnimus, H. Girschick, P. Tas, E. Flory, M. Heinklein and C. Jassoy, *J Membr Biol*, 2000, **175**, 181-189.
44. S.K. Huang, E.S. White, S.H. Wettlaufer, H. Grifka, C.M. Hogaboam, V.J. Thannickal, J.C. Horowitz and M. Peters-Golden, *FASEB J.*, 2009, **23**, 4317–4326.
45. E. Brauchle, S. Thude, S. Y. Brucker and K. Schenke-Layland, *Sci Rep*, 2014, **4**, 4698.
46. Y.M. Michelacci, *Brazilian Journal of Medical and Biological Research*, 2003, **36**, 1037-1046.
47. N. N. Fathima and A. Dhathathreyan, *Int J Biol Macromol*, 2009, **45**, 274-278.
48. Y. Hashimoto, S. Funamoto, S. Sasaki, T. Honda, S. Hattori, K. Nam, T. Kimura, M. Mochizuki, T. Fujisato, H. Kobayashi and A. Kishida, *Biomaterials*, 2010, **31**, 3941-3948.

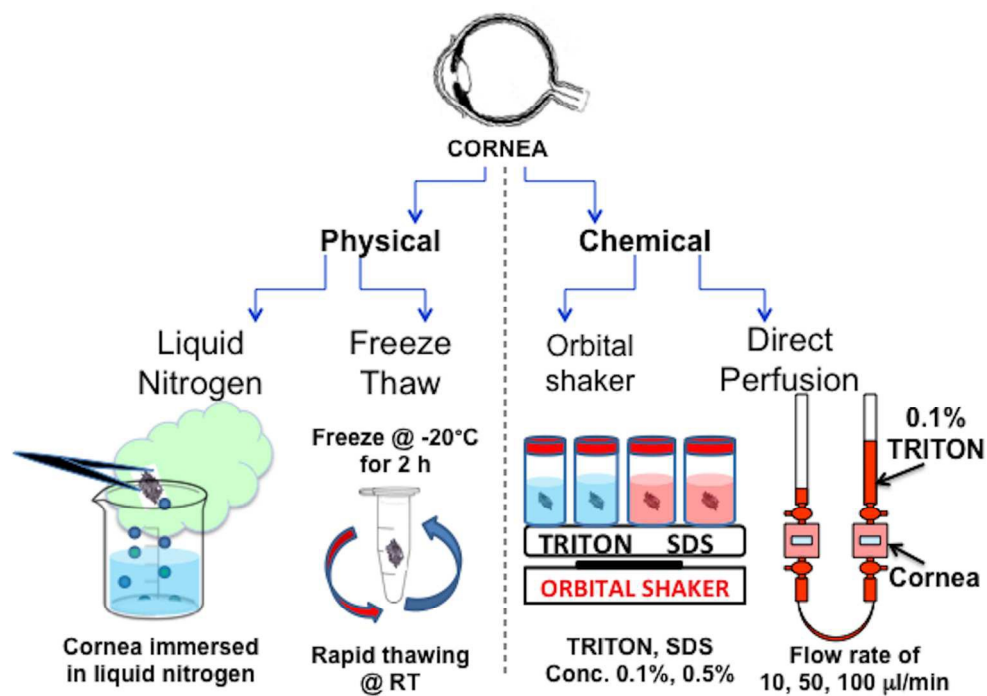


Fig. 1 Schematic representation of the four different methods used for the decellularization of goat cornea. 213x150mm (300 x 300 DPI)

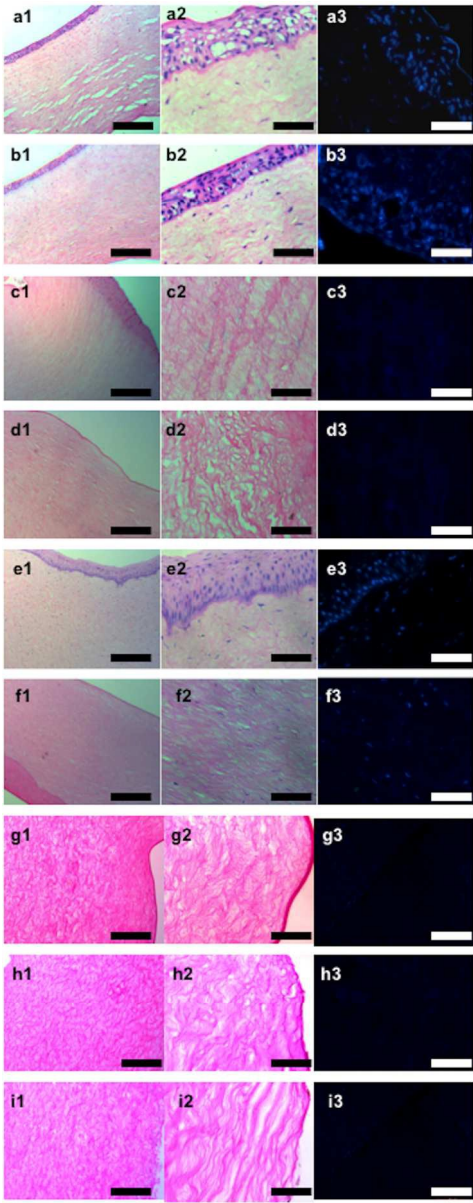


Fig. 2 Histological analysis of decellularized cornea to compare the efficiency of the various cell removal techniques. Left panel: Light micrographs of H&E (Scale 200  $\mu\text{m}$ ); Centre: Higher magnification H&E (Scale 50  $\mu\text{m}$ ); Right panel: Fluorescence images of DAPI (Scale 50  $\mu\text{m}$ ). Top to bottom: Physical methods; (a1-a3): liquid nitrogen, (b1-b3): freeze-thaw, Chemical methods; (c1-c3): 0.1% SDS in orbital shaker, (d1-d3): 0.5% SDS in orbital shaker, (e1-e3): 0.1% TRITON in orbital shaker, (f1-f3): 0.5% TRITON in orbital shaker, TRITON in perfusion chamber at different flow rates; (g1-g3): 10  $\mu\text{l}/\text{min}$ , (h1-h3): 50  $\mu\text{l}/\text{min}$ , (i1-i3): 100  $\mu\text{l}/\text{min}$ .  
119x303mm (300 x 300 DPI)

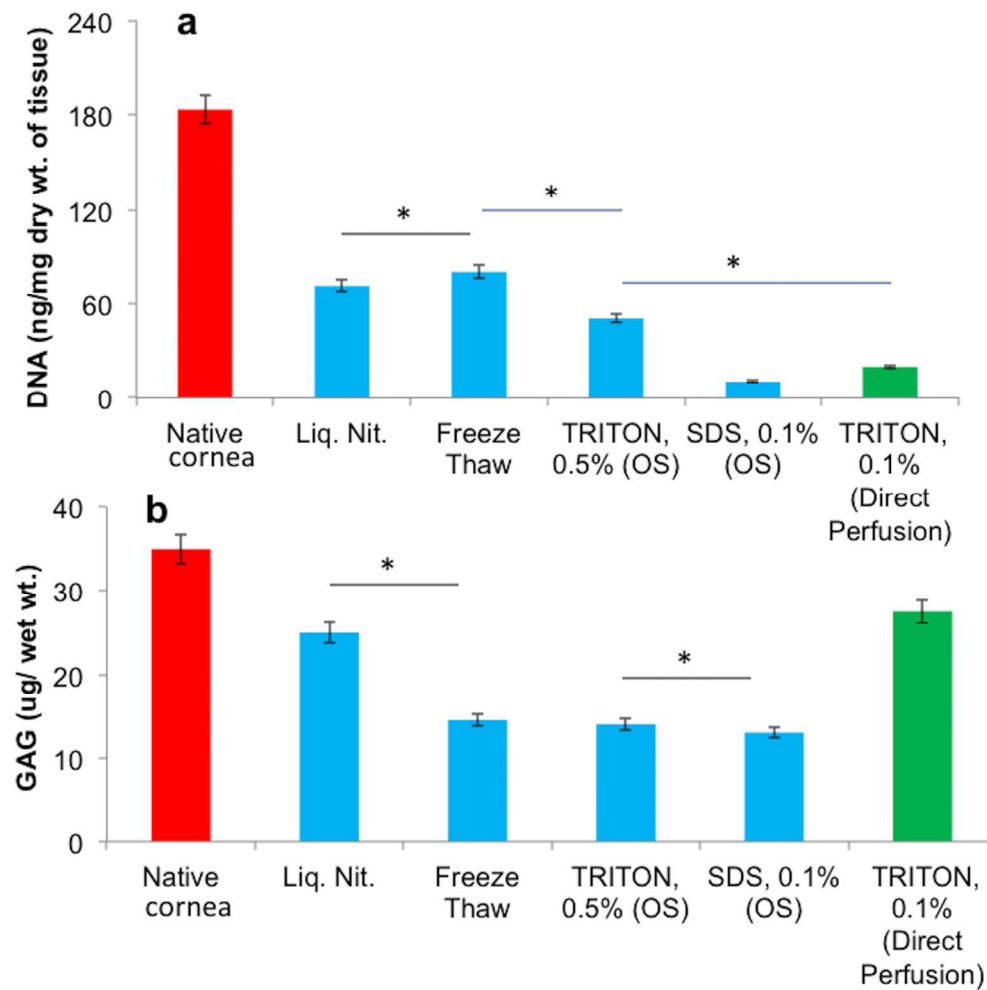


Fig. 3 Biochemical analysis of decellularized cornea; (A) GAG content and (B) total DNA content (\*  $p < 0.01$ ,  $n = 3$ ). GAG analysis revealed that TRITON, 0.1% (Direct Perfusion) is most efficient in preserving the ECM content of the corneas. For DNA analysis, both SDS 0.1% (OS) and TRITON, 0.1% (Direct Perfusion) methods gave satisfactory results compared to other methods. Hence TRITON, 0.1% (Direct Perfusion) method decellularized cornea as well as preserved the native extracellular matrix components of the corneal tissue. Abbreviation: ECM-Extracellular matrix, OS - Orbital shaker.

190x189mm (300 x 300 DPI)

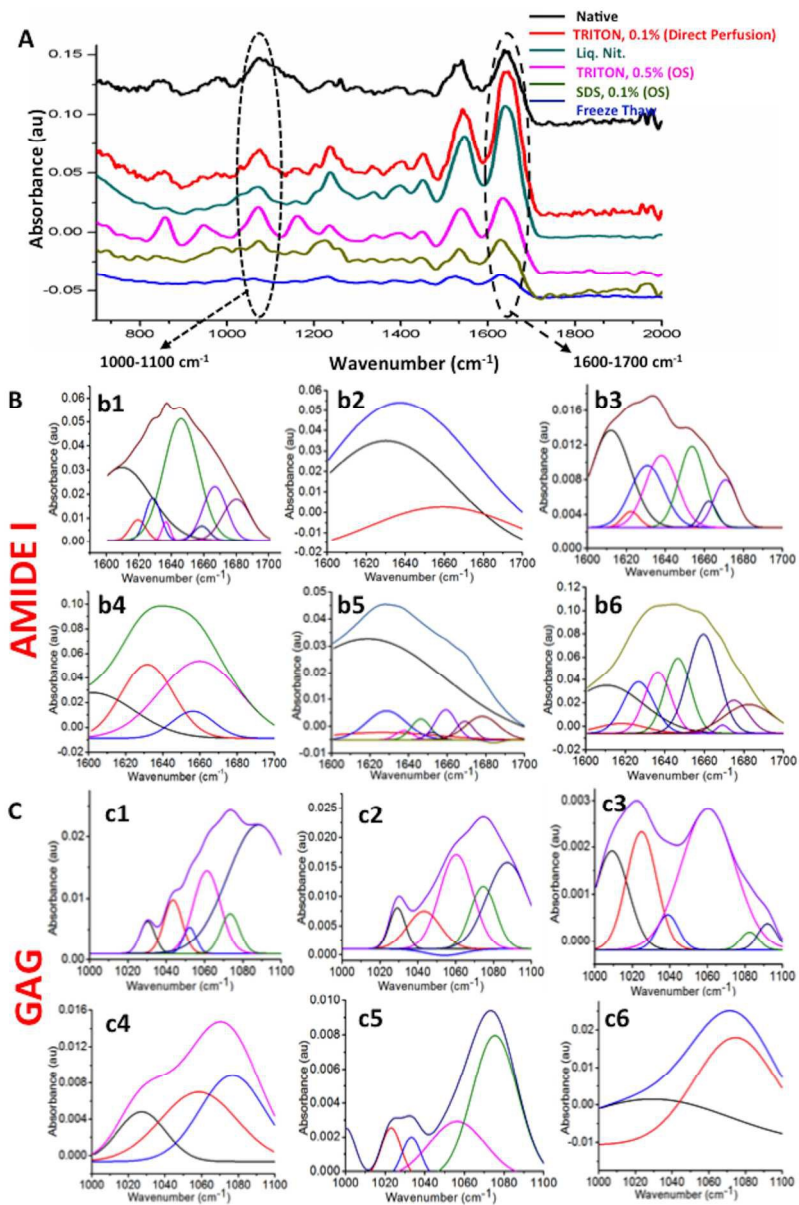


Fig. 4 (a) ATR-FTIR of decellularized and native corneas. Deconvoluted spectra of 1600-1700 cm<sup>-1</sup> spectral interval, (b1) Native cornea; (b2) TRITON, 0.1% (Direct Perfusion); (b3) Liq. Nit.; (b4) Freeze Thaw; (b5); (b6) TRITON (0.5%), (OS). Deconvoluted spectra of 1000-1100 cm<sup>-1</sup> spectral interval, (c1) Native cornea, (c2) TRITON, 0.1% (Direct Perfusion), (c3) Liq. Nit., (c4) Freeze Thaw, (c5) SDS, 0.1% (OS), (c6) TRITON (0.5%) (OS). Abbreviation: Liq. Nit - Liquid Nitrogen.  
166x250mm (300 x 300 DPI)



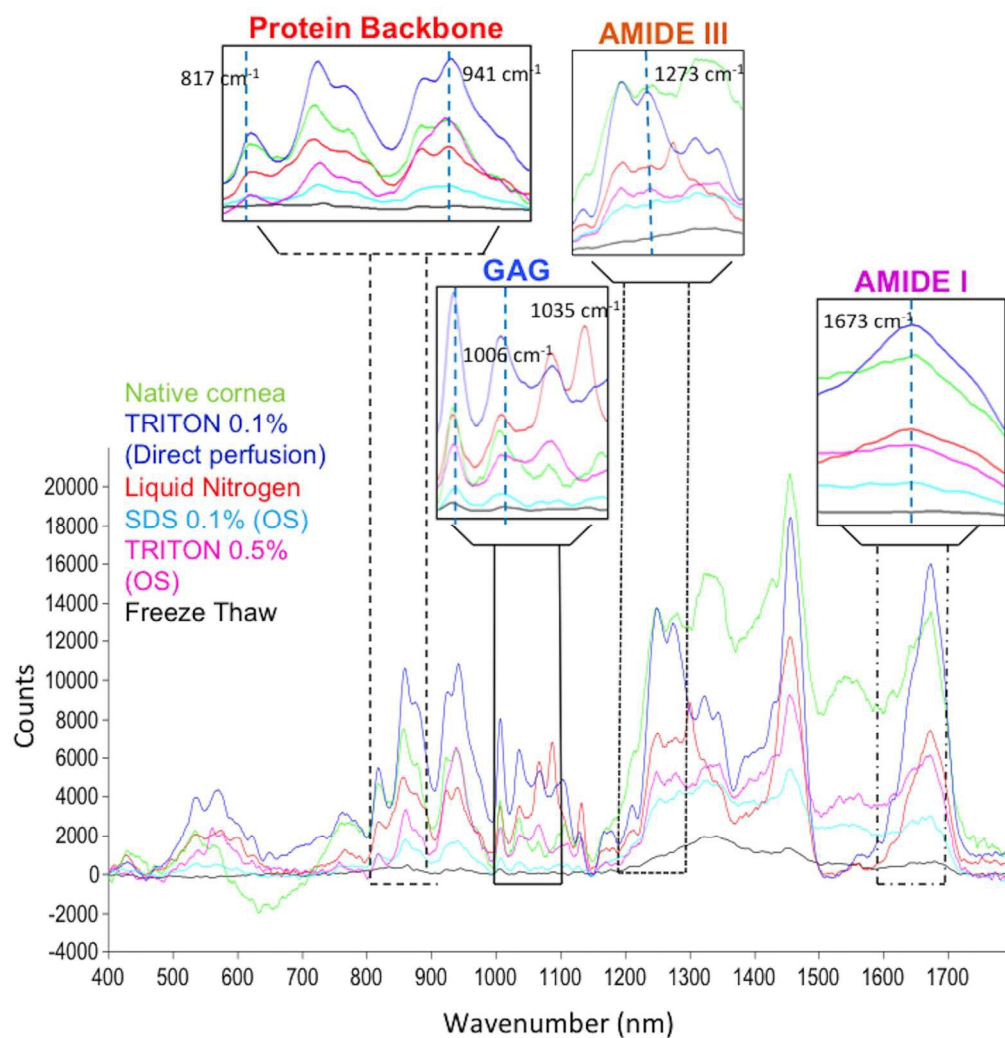


Fig. 5 Raman spectra of decellularized corneas excited at 488 nm. The Amide I (1600-1700  $\text{cm}^{-1}$ ), Amide III (1200-1300  $\text{cm}^{-1}$ ), GAG (1000-1100  $\text{cm}^{-1}$ ) and Protein backbone (800-900  $\text{cm}^{-1}$ ) regions are zoomed in the insets to show the corresponding peaks elucidating the corneal chemistry.  
183x189mm (300 x 300 DPI)

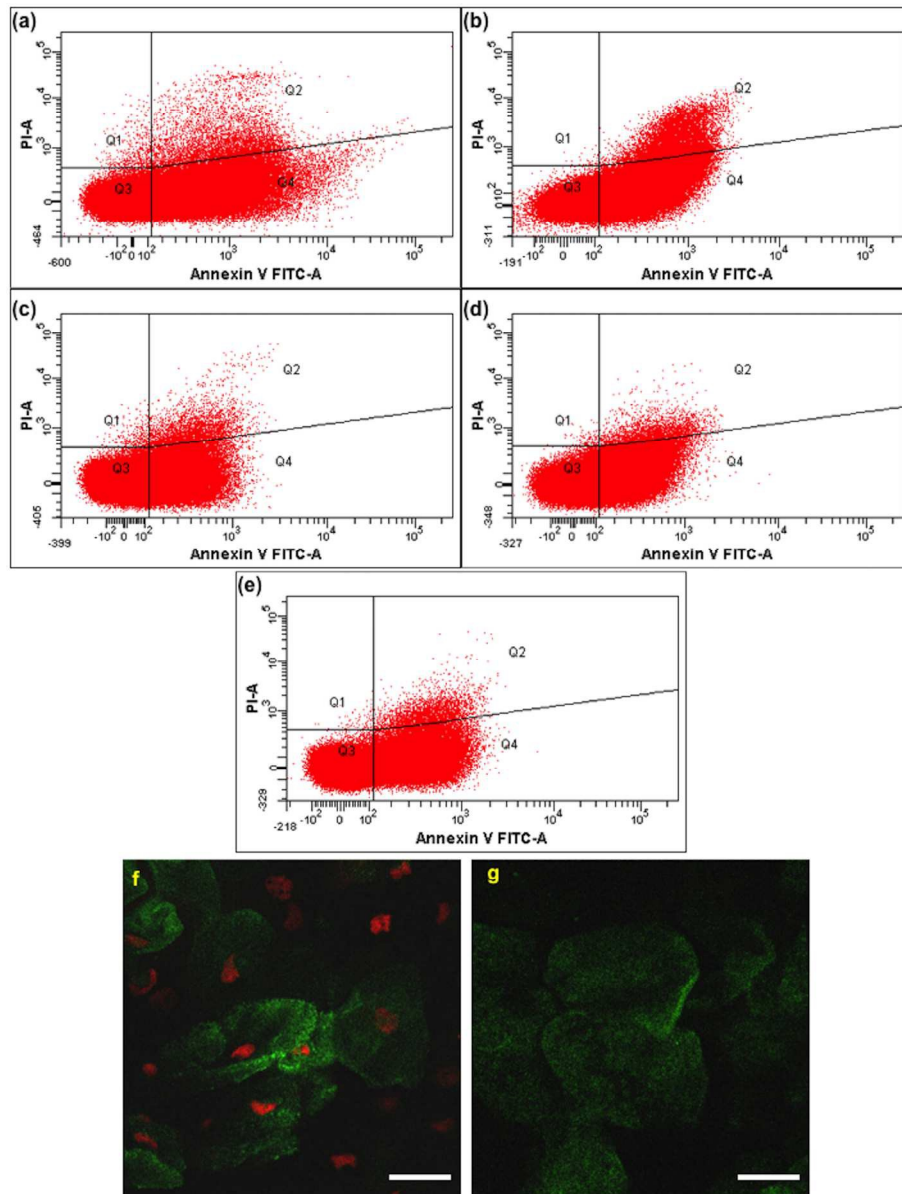


Fig. 6 FACS scatterplots of stromal cells isolated from decellularized cornea processed by different methods and stained with annexin V (green) and propidium iodide (red); (a) Native, (b) Liq. Nit., (c) Freeze Thaw, (d) TRITON, 0.1% (Direct Perfusion), (e) TRITON, 0.1% (OS). Representative fluorescent images (scale 10  $\mu$ m) of (a1) necrotic cells, (a2) apoptotic cells.  
170x223mm (300 x 300 DPI)

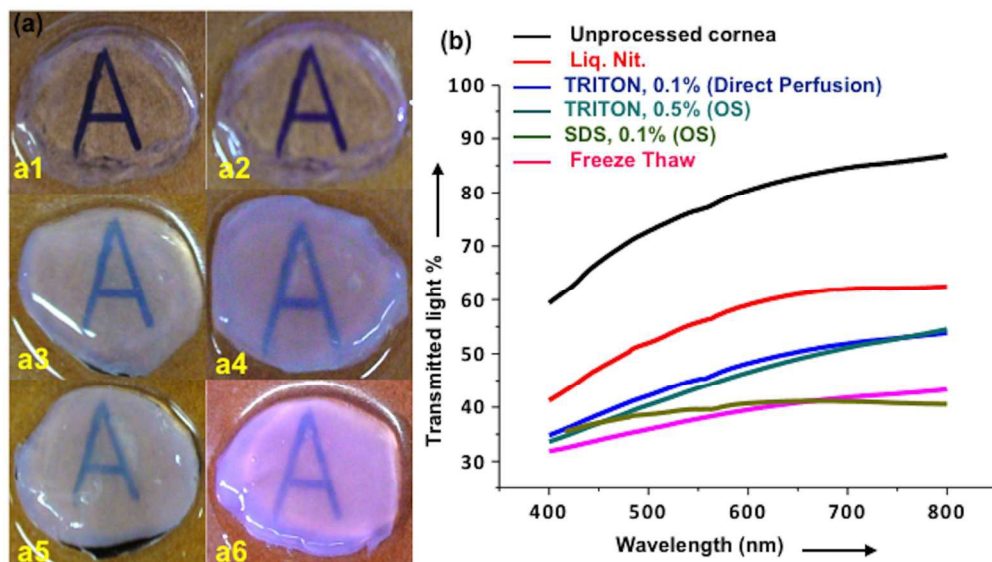


Fig. 7 (A) Transparency of cornea; (a1) untreated, (a2) treated with liquid nitrogen, (a3) TRITON (0.1%)-direct perfusion, (a4) TRITON (0.5%)-Orbital shaker, (a5) freeze-thaw and (a6) SDS (0.1%)-Orbital shaker. (B) Transmittance measurements of decellularized cornea using different methods. 210x119mm (300 x 300 DPI)

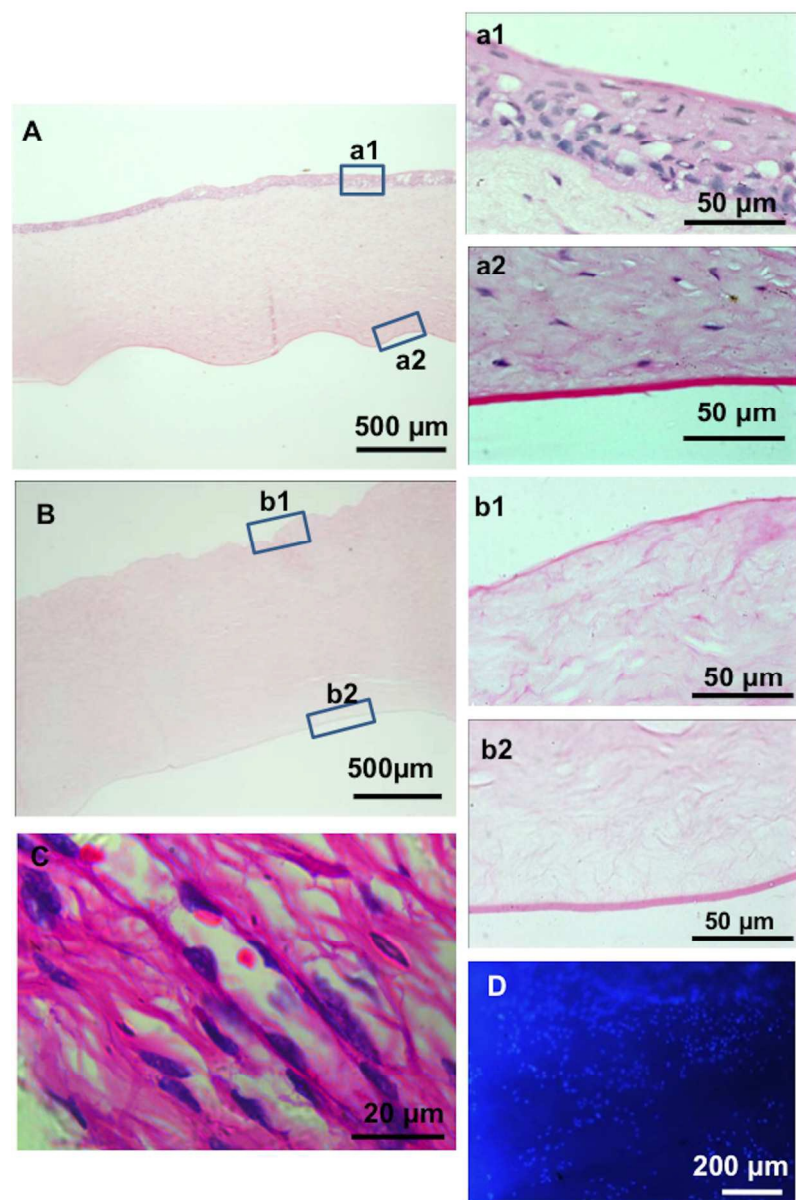
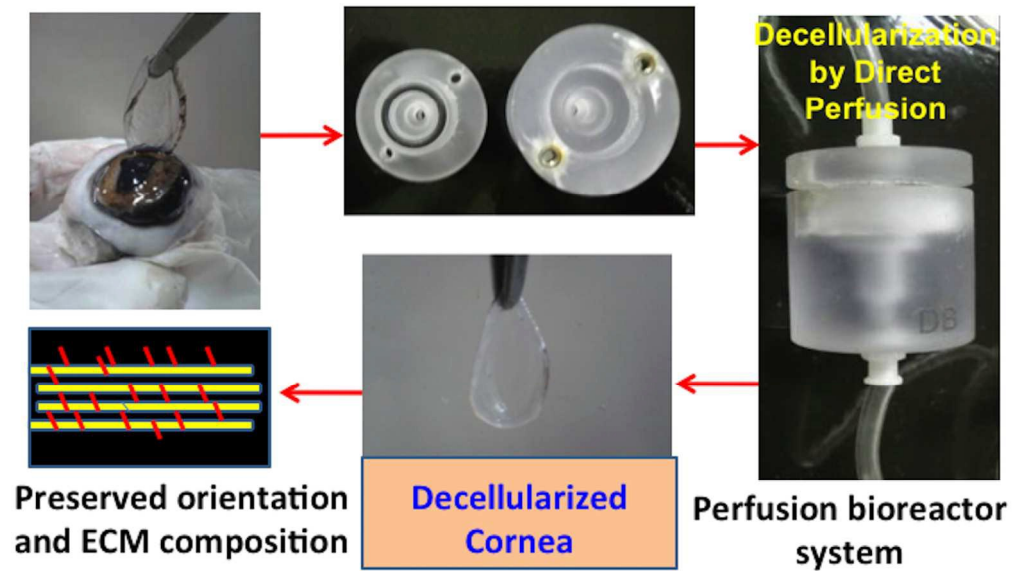


Fig. 8 H&E staining: A; Native cornea displaying intact Bowman's (a1) and Descemet's membrane (a2), B; Decellularized cornea with TRITON (0.1%)- direct perfusion at 10  $\mu$ l/min with intact Bowman's (b1) and Descemet's membrane (b2), C; Cells uniformly dispersed into the matrix after recellularization and DAPI staining (D) of recellularized corneal matrix obtained from direct perfusion showing the presence of goat keratocytes seeded on decellularized corneal matrices.  
158x240mm (300 x 300 DPI)



174x99mm (300 x 300 DPI)